Genetic diversity and phenotypic plasticity of AHL-mediated Quorum sensing in environmental strains of Vibrio mediterranei

Léa Girard, François Lantoine, Raphaël Lami, Florence Vouve, Marcelino Suzuki, Julia Baudart

Genetic Diversity and Phenotypic Plasticity of AHL Mediated Quorum Sensing in Environmental Strains of *Vibrio mediterranei*

Léa Girard[1], François Lantoine[2], Raphael Lami[1], Florence Vouvé[3,1], Marcelino T. Suzuki[1] and Julia Baudart[1*]

[1]Sorbonne Université, CNRS, Laboratoire de Biodiversité et Biotechnologies Microbiennes LBBM, F-66650 Banyuls sur Mer, France.

[2]Sorbonne Université, CNRS, Laboratoire d'Ecogéochimie des Environnements Benthiques, LECOB, F-66650 Banyuls/Mer, France.

[3]Université Perpignan Via Domitia, Laboratoire Biocapteurs-Analyses-Environnement (B.A.E), F-66860 Perpignan, France.

[*]**Correspondance**: J. Baudart, Sorbonne Université, CNRS, Laboratoire de Biodiversité et Biotechnologies Microbiennes, LBBM, Observatoire Océanologique, F-66650 Banyuls/Mer, France. E-mail :baudart@obs-banyuls.fr, Tel: +33468887368

Keywords: Quorum sensing, *N*-acyl-homoserine lactone, *Vibrio mediterranei*, Phenotypic plasticity

Running title: Phenotypic Plasticity of AHL Mediated Quorum Sensing

Funding: This work was supported by a Ph.D. grant from doctoral school ED227 Sciences de la Nature et de l'Homme : évolution et écologie associating Sorbonne Université and Museum National d'Histoire Naturelle (MNHN), France.

Conflict of interest: The authors declare no conflict of interest.

To be submitted to **ISME Journal** - Subject Category **Microbes-microbes and microbe-host interactions**

ABSTRACT

N-Acyl-Homoserine Lactone (AHL) mediated Quorum Sensing (QS) is one of the most studied social behavior among *Proteobacteria*. However, despite the current knowledge on QS-associated phenotypes such as bioluminescence, biofilm formation or pathogenesis, the characterization of environmental factors driving QS in realistic ecological settings remains scarce. We investigated the dynamic of AHL and AHL-producing *Vibrio* among 840 strains isolated fortnightly from the Salses-Leucate Mediterranean lagoon in Spring and Summer 2015 and 2016. *Vibrio* isolates were identified by *gyrB* gene and genome sequencing and AHL production was investigated by a biosensors-based UHPLC-HRMS/MS approach. Our results revealed, for the first time, a succession of *V. mediterranei* isolates with different AHL-production phenotypes over time and this dynamic lies with a single genotype (Average genomic Nucleotide Identity (ANI) > 99.9). A multivariate DistLM analysis revealed that the temporal variation of *V. mediterranei* QS phenotypes was explained by environmental variables at 83.4%. Overall, our results suggest that isolates of a single genotype are able to change their QS phenotypes in response to environmental conditions, highlighting phenotypic plasticity of bacterial communication in the environment.

INTRODUCTION

Bacterial communities inhabiting marine coastal areas are subjected to rapid and somewhat unpredictable changes in their environment (Lennon and Jones, 2011). In order to cope with these changes, bacteria implement flexible strategies supporting a certain degree of phenotypic plasticity (Agrawal, 2001; West-Eberhard, 2003; Chevin *et al.,* 2010). *Vibrio* are well-known for their capacity of rapid physiological adaptation in response to changing environmental conditions, making them highly dynamic over short-term and seasonal scales (Takemura *et al.,* 2014). These opportunistic bacteria are sensitive to unfavorable conditions by switching from an active free living state into a "dormant" viable but not culturable (VBNC) phenotype, or by colonizing viscous surfaces such as biofilms (Whitesides and Oliver, 1997; Li *et al.,* 2014; Chimetto Tonon *et al.,* 2015; Vezzulli *et al.,* 2015). When favorable conditions reappear their high reactivity allow them to colonize new substrate and to be part of the microbial community associated with zooplankton, phytoplankton, and marine vertebrates and invertebrates (Heidelberg *et al.,* 2002; Ben-Haim, 2003; Soto *et al.,* 2009; Wendling and Wegner, 2015).

In the past decades, our vision of bacterial communities has significantly changed and microbial cells are no longer considered to behave individually but rather to act socially (West *et al.,* 2006, 2007; Goo *et al.,* 2015). It is now clear that microorganisms perform social behaviors, synchronizing the expression of functional genes at high cell-density by sensing their surrounding environment. This mechanism is generally known as Quorum sensing (QS) (Fuqua *et al.,* 1994) and Type 1 auto-inducers (AI-1) also called *N*-acyl-homoserine lactones (AHL) are important signal molecules for the communication between close relative members of *Proteobacteria*. Among *Vibrio* species, most of the studies are highlighting the processes controlled by QS, i.e. QS-associated phenotypes, such as bioluminescence and symbiosis (Bassler *et al.,* 1994; Schwartzman and Ruby, 2015), biofilm formation (Hammer and Bassler,

2003), toxin production or expression of virulence factors (Zhu *et al.,* 2002; Natrah *et al.,* 2011; Ha *et al.,* 2014). *In vitro* studies have demonstrated the involvement of QS in the "resuscitation" of viable but non-culturable (VBNC) *Vibrio* cells (Bari *et al.,* 2013; Ayrapetyan *et al.,* 2014). However, Platt and Fuqua (2010) presented the QS process itself (i.e. the production of signal molecules), as impacted by multiple aspects of natural environments, and in support to this idea, some studies on AHL biosynthetic pathways have suggested that any environmental factor likely to affect the primary metabolism of bacteria can modify his spoken "language" (Hoang *et al.,* 2002; Gould *et al.,* 2006). Finally, several studies have reported heterogeneous AHL Production Phenotypes (APP) among different isolates of a single *Vibrio* species, i.e. the production of different sets of AHLs, according to their origin (Buchholtz *et al.,* 2006; García-Aljaro *et al.,* 2012; Purohit *et al.,* 2013; Rasmussen *et al.,* 2014).

Despite all this previous knowledge, the question of whether AHL Production Phenotypes (APP) form coherent populations in the environment, show temporal dynamics, or respond to different environmental conditions, remains largely underexplored. Therefore, in the present study we investigated over a two-year period, the temporal dynamics of AHL-producing *Vibrio* isolates from a French Mediterranean lagoon and evaluated the possible links between phenotypic plasticity of AHL production and environmental conditions.

MATERIALS & METHODS

Sample collection

A two-years study was carried out during Spring and Summer (April to July) 2015 and 2016, at one sampling site in the South basin of the Salses-Leucate lagoon, on the Mediterranean coast of France, (42° 50'54.6" N, 3°00'08.7" E; **Fig S1**). Surface water was

collected in sterile bottles and pre-filtered through a 50 µm mesh. Plankton was collected using a 5 min horizontal tow at 2 knots of a 50 µm plankton net (30 cm diameter, 1 m length, 500 mL cod-end), and all samples were processed within three hours. For each sampling date, triplicate plankton aliquots of 15 mL were fixed with 4% neutral Lugol's solution (0.68 % potassium iodide and 0.34 % iodine in distilled water) and stored in the dark at 4°C. Taxonomic identification and enumeration were performed within two months. Surface temperature (°C), salinity (psu), dissolved oxygen (DO, % saturation), conductivity (mS/cm) and pH were recorded at each sampling date using a HQ40d multiparametric profiler (Hach). Physico-chemical parameters, as well as pigments were analyzed using standard methods (the methodological details can be found in **Table 1)**.

Large phytoplankton and picoplankton counts

Phytoplankton counts were carried out with an Olympus IMT inverted microscope in 5, 10, 25 or 50 ml plate chambers using the Utermöhl method updated by Karlson and collaborators (Karlson *et al.,* 2010). Replicates of different volumes were counted according to the size and the abundance of the cells. Small sized species were mainly counted in diagonal transects at 300x magnification and for the large or less abundant species half or whole chambers were scanned at 100x and 40x magnification. A minimum of one hundred total cells were counted for each enumeration. Different settling times were applied according to chamber volume in a temperature-controlled room (Karlson *et al.,* 2010). For picoplankton enumeration, seawater samples were collected (1.5 ml in triplicate fixed on board with 1% glutaraldehyde and then quickly frozen at -80°C). The picoplankton abundances, including cyanobacteria (mainly represented by *Synechococcus*), pico- and nano-eukaryotes, and cryptophytes were measured with a FACSCanto II (Becton Dickinson) flow cytometer. The analyses were performed within one month after the sampling. Heterotrophic bacterial cells were stained with SYBR-Green I (Molecular Probes) before flow cytometry analysis.

Reference beads (Fluoresbrite YG Microspheres, calibration grade 1.00 µm and 10.00 µm, PolySciences, Inc) were added to each sample before acquiring the data. Each planktonic group was analysed according to Marie *et al.* (2014) with the Cell Quest Pro software (Becton Dickinson), in logarithmic mode, to separate the populations based on their scattering and fluorescence signals.

Vibrio isolation and characterization

For the enumeration of *Vibrio*, water samples (0.1, 1, 10 mL) were filtered onto 0.45 µm pore-size nitrocellulose filters (Millipore, 47 mm), plated on the selective medium thiosulfate-citrate–bile–sucrose (TCBS) (Pfeffer and Oliver, 2003) and incubated 24h at 20°C. *Vibrio* strains were isolated from two fractions: less than 50 µm assumed to mostly represent *Vibrio* in the water column and greater than 50 µm corresponding large phytoplankton and zooplankton-associated *Vibrio*. The <50 µm fraction consisted of 20 L of 50 µm prefiltered water further concentrated using a hollow fiber filter HF80S (Hemoflow, Fresenius Medical Care). The concentrate was back-washed with 500 mL of a wash solution (0.01% sodium hexametaphosphate, and 0.5% Tween 80; Sigma-Aldrich). The >50 µm fraction consisted of a plankton net tow concentrate splited into five subsamples of 15 mL and homogenized by gentle sonication for 5 min in order to unbind attached bacteria. For both fractions, a ten-fold serial dilution was made in artificial seawater and 100 µL of each was plated in triplicate on TCBS agar. Thirty colonies by fraction and by sampling date were randomly picked using a gridded Petri dish.

Isolate identification

A total of 840 isolates were identified based on *gyrB* gene sequences. The PCR was performed using colony cells and amplification reactions consisted of 12.5 µL of Kappa2G Master Mix (KAPA2G Fast Hotstart ReadyMix PCR kit, KapaBiosystems), 6.25 µL of 10

mM $MgCl_2$ and 1.25 µL of each of universal *gyrB* primers UPIE (5'GAAGTCATCATGACCGTTCTGCAYGCNGGNGGNAARTTYRA 3') and UP2AR (3'AGCAGGGTACGGATGTGCGAGCCRTCNACRTCNGCRTCNGYCAT 5') (Le Roux *et al.,* 2004). The PCR conditions were slightly optimized for the KAPA2G Fast DNA Polymerase and were as following: a 5 min initial denaturation step at 95 °C, followed by 40 cycles at 95 °C for 15 sec, 60 °C for 30 s and 72 °C for 30 s, and a final elongation step of 2 min at 72 °C. PCR products were sent to Macrogen Europe for sequencing using the dideoxy-termination (Sanger) reaction with the primer *gyrB* UP1S (5'GAAGTCATCATGACC-GTTCTGCA3') (Yamamoto and Harayama, 1995) to obtain sequences around 800 bp length.

Detection of QS-active isolates

The methodological approach for the screening of AHL producers and the identification of AHL compounds by Ultra High Performance Liquid Chromatography coupled with High Resolution tandem Mass spectrometry UHPLC-HRMS/MS were strictly identical to those previously described in Girard *et al.,* (2017). Briefly, two biosensors were used, *Pseudomonas putida* (pKR-C12) for long acyl-side chained AHLs (C8-C18) and *Escherichia coli* (pJBA-132) for short acyl-side chained AHLs (C6-C10) (Girard *et al*., 2017). Isolates were tested, in triplicate, on each biosensor immediately after isolation from the environmental samples and also before mass spectrometry analysis.

Genetic and genomic characterization of V. mediterranei isolates

The genetic diversity of *V. mediterranei* isolates was evaluated by ERIC-PCR (Rivera *et al*., 1995). Briefly, genomic DNA from 253 isolates was obtained by cellular lysis (3 quick cycles of liquid nitrogen freeze/70°C thaw) and DNA concentrations were measured spectrophotometrically in order to dilute each lysate at 100 ng/µL. The ERIC-PCR reactions were performed using previously described protocols employing the ERIC1 and ERIC2

primers (Hulton *et al.,* 1991; Khan *et al.,* 2002). PCR amplifications were performed with the GoTaq G2 Flexi polymerase (Promega) and fingerprinting profiles were visualized using a Typhoon FLA 9000 imager (GE Life Sciences). Gel images analysis were performed using the GelJ software (Heras *et al*., 2015). For whole genome sequencing, genomic DNA of two *V. mediterranei* isolates (17 LN0615E and 21 LS0615E) was obtained with a classical CTAB-β-mercaptoethanol extraction protocol and sent for DNA sequencing (Illumina MiSeq) by Mr DNA (Shallowater, TX, USA) as described by Doberva *et al.,* (2014). Genomes were automatically annotated using the RAST server (Aziz *et al.,* 2008).

Multivariate analyses

A preliminary PERMANOVA analysis (Anderson, 2001a) was used to test for significant differences among *Vibrio* assemblages and *V. mediterranei* APP between the two size fractions (<50µm and > 50µm). As the results indicated that there were no significant differences between the two size fractions the remainder of the analysis was then performed by pooling the counts from both fractions. The relationships between G1 *V. mediterranei* assemblage (i.e. the abundance of each AHL production phenotypes over time, Square-root transformed and Bray-Curtis distance matrix) and all measured environmental variables (Normalization and Euclidean distance matrix) were investigated using a Distance Based Linear Model (DISTLM) (McArdle and Anderson, 2001). In order to visualize if the temporal variations of G1 phenotypes co-occurred with specific phytoplankton taxa, we conducted a second step of analysis consisting of a Principal Component Ordination (PCO) of G1 phenotypes using phytoplankton counts (Square-root transformed and Bray-Curtis distance matrix) as predictor variables (non-parametric Spearman rank correlation). All the multivariate analyses were performed using PRIMER v.7 and its add-on package PERMANOVA + (Anderson, 2001a; Anderson, 2001b; McArdle and Anderson, 2001).

RESULTS

Phenotypic and Genetic temporal variation of V. mediterranei isolates

The partitioning of *Vibrio* isolates, between the water column (<50 µm) and plankton (>50 µm), was monitored during spring and summer 2015/2016 and a total of 840 isolates were identified as *Vibrio* spp. We did not observe differences in *Vibrio* assemblages between the fractions over time (data not shown, PERMANOVA, *p value* = 0.904; the temporal variation of the total *Vibrio* spp. can be found in **Fig S2**). Isolates identification, based on *gyrB* gene sequences, from both size fractions, showed a seasonal dynamic of *V. mediterranei* isolates (**Figure 1**) in particular for 2016, starting from 0-28% of total *Vibrio* isolates during spring and increasing gradually to up to 97% (Summer 2016). Interestingly, the phenotyping of these isolates, under identical culture and screening conditions, revealed a temporal variation of AHL production phenotypes (APPs) among time. APPs varied for example from strains producing only long chain AHLs ($F117^{+}/MT102^{-}$) to those producing long and short chain AHLs ($F117^{+}/MT102^{+}$) in 2015, or from a predominance of isolates exhibiting no production ($F117^{-}/MT102^{-}$) to an exclusive production of long chain AHLs ($F117^{+}/MT102^{-}$) in 2016 (**Figure 1B**).

In order to determine if these phenotypic changes were related to a shift between different genotypes of *V. mediterranei*, we used ERIC-PCR (Rivera *et al.,* 1995) to genotype 253 *V. mediterranei* strains. A total of 22 genotypes were identified, G1 to G22 (i.e. **Figure 1A** and **Supplementary Figure 3**) and remarkably, 83% of the *V. mediterranei* isolates, over the two years period, belonged to Genotype 1 (G1). To implement the genetic characterization of *V. mediterranei* G1 isolates and to better understand the genetic basis of this phenotypic variations, we obtained a draft whole genome sequence for two strains with different phenotypes (17LN 0615E with $F117^{+}/MT102^{-}$ phenotype and 21LN 0615E with

212 F117^{+}/MT102^{+} phenotype, NCBI accession numbers NZ_NWTN00000000 and
213 NZ_NWTO00000000, respectively). A comparison between these genomes yielded an ANI
214 value of 99.96%. Since, as previously proposed, two strains can be considered identical if they
215 have a ANI value >99.9% (Snitkin *et al.,* 2012; Olm *et al.,* 2017), we consider that we
216 observed a phenotypic plasticity of AHL production within a single strain of *V. mediterranei*.
217 To summarize, we observed in 2016, the predominance of a single strain of *V. mediterranei,*
218 up to 97% of the total cultivable *Vibrio* spp., showing different APPs over time.

219 ***AHL characterization of G1 V. mediterranei APP***

220 In order to confirm that the observed APPs indeed corresponded to different AHL
221 patterns, we analyzed the produced AHLs among two representative isolates of each
222 phenotype (F117^{+}/MT102^{-}) and (F117^{+}/MT102^{+}) by UHPLC-HRMS/MS. AHL
223 characterization was carried out according to the procedure described in Girard *et al.*, 2017,
224 briefly, "anticipated" AHLs were identified by comparison with their corresponding standards
225 (**Table S8**) while "unanticipated" AHLs, without commercially available standards, were
226 identified based on their fragmentation patterns, predicted retention time and molecular weight
227 (i.e. **Table S6 and S7**). A total of 13 AHLs were detected and 8 were common to the four
228 isolates, namely OH-C10-HSL, oxo-C10-HSL, OH-C11-HSL, OH-C12-HSL, oxo-C12-HSL,
229 C12-HSL, C13-HSL and oxo-C13-HSL (**Fig. 2** and **Figure S4**). Three short chain AHLs, C6-
230 HSL, oxo-C6-HSL, and oxo-C8-HSL were putatively identified as being responsible for the
231 F117^{+} /MT102^{+} phenotype. Interestingly, we observed that two long chain AHLs, oxo-C11-
232 HSL and C14-HSL, were produced by the (F117^{+}/MT102^{-}) isolates but were not detected in
233 the (F117^{+}/MT102^{+}) isolates. Summarizing, the AHL analysis confirmed that the different
234 APPs detected by the biosensors are producing different AHLs patterns, with (F117^{+}/MT102^{-})
235 producing long acyl-side chains and (F117^{+}/MT102^{+}) producing long plus short acyl-side
236 chains AHLs.

237 ***Genetic basis of AHL production***

238 One possibility to explain these different APPs with highly similar genomes would be
239 that these differences were carried by different AHL synthase genes. Thus, we searched for
240 AHL synthase genes in the two genomes of *V. mediterranei* G1 strains and a LuxI/LuxR QS
241 system was found. However, as it has been shown that some *Vibrio* species can harbor two
242 AHL production pathways (LuxI/R and LuxM/N) we also searched for other putative *N*-
243 acetyltransferases in our two genomes. The comparison between the two strains (17 LN0615E
244 and 21 LS0615E) revealed a 100% protein identity for the AHL synthase LuxI (accession
245 numbers PRQ68803.1 and PCD89229.1, respectively) but also for the 15 putative N-
246 acetyltransferases (**Table S9**). Altogether these results suggest that the differences observed in
247 terms of AHL production patterns are not explained by different presumptive AHL synthases.

248 ***Factors affecting the dynamic of G1 - AHL production phenotypes***

249 To investigate the relationships between the dynamic of the APPs among G1 strains
250 and the environmental variables we conducted a distance based linear modeling approach
251 (DistLM). A total of 7 variables explained 83.4% of the temporal variation of G1 APPs, and
252 among those, phosphates concentration was the variable with the highest explanatory value
253 (37.4 %) and ammonium concentration the lowest with 4.5% (**Figure 3** and sequential tests,
254 **Table 2**). Axis 1 (db RDA1) represented essentially a gradient in abundance of the genotype
255 varying from high abundances at the left-end to low abundances or no counts at the right-end
256 (July 2015 and April/May 2016). Samples with high counts of *V. mediterranei* G1 were
257 associated with higher conductivity (an integrated measure of higher temperature and salinity),
258 total dissolved nitrogen, and low phaeophytin concentrations, while an inverted trend was
259 observed for samples with low counts or where *V. mediterranei* G1 was not retrieved. Axis 2
260 (db RDA2) reflected the distribution of the different APPs. A peak of phosphates and nitrites

were associated with an increase of non AHL producers in the higher end of the axis. As the ($F117^{+}/MT102^{-}$) phenotype was dominant at dates with high counts of G1 isolates, the same parameters are linked to counts of the ($F117^{+}/MT102^{-}$) phenotype at the lower end of db RDA2 axis.

A principal coordinates analysis (PCO) was performed in order to visualize which phytoplankton species co-occurred with the different APP (**Fig 4**). As observed in the db RDA1, Axis 1 (PCO1) reflected the gradient in G1 abundances among the sampling dates with the lowest counts of G1 in the right-end (July 2015 and April/May 2016) and where *picoeukaryotes, Cryptophyta,* unidentified *nanoeukaryotes, Dinophysis* sp. and *Prorocentrum micans* were present in their highest abundances. In the left-end of PCO axis 1 were samples with the highest G1 counts (June 2015 and June/July 2016) associated to the highest counts of *Grammatophora* sp. and *Scrippsiella* sp. and bacteria abundances. Axis 2 (PCO2) mostly separates dates based on the presence of *V mediterranei* G1 AHL producers and non-producers. While *Gonyaulax* sp*., Amylax* sp*.,* seemed to be associated to dates with the highest counts of non-producers (2016/06/21), *Cyanobacteria* and *Pyrophacus* sp. abundances were linked to AHL producers.

Discussion

It is well known that the ability of *Vibrio,* as well of other gram negative bacteria, to survive by making biofilms, to infect hosts, to modify their metabolism or to enter into a VBNC state, is modulated by QS (Ayrapetyan *et al.,* 2014; Bondí *et al.,* 2014; Goo *et al.,* 2015; Persat *et al.,* 2015). In addition to the fact that QS allows bacteria to sense their number and coordinate their actions, the variability of auto-inducers production might offer an advantageous response to adapt their actions according to environmental fluctuations.

In order to survive in changing environment, bacteria have evolved to set up various adaptive responses. Phenotypic plasticity is one of them and it reflects the direct influence of the environment on the development of individual phenotypes, in other words, bacteria can adapt to environmental selective pressures to maintain their own fitness. Phenotypic diversity of QS systems has already been described for different strains of a single *Vibrio* species (Buchholtz *et al.*, 2006; Joelsson *et al.*, 2006; García-Aljaro *et al*., 2012; Purohit *et al.*, 2013) and temporal changes in AHLs production during the development of natural biofilm including *Vibrio* species as been shown (Huang *et al.,* 2009). However, the scope of these earlier studies did not show clear evidence of QS phenotypic plasticity. Our results show a clear short-term temporal variation in APPs among environmental isolates of a single *Vibrio* species (*V. mediterranei*) that were remarkably grouped in a single genotype (G1) based on *gyrB* sequences, ERIC-PCR and genomic analysis. This change of AHL production patterns, was temporally coherent and in some cases reached the near totality of *Vibrio* isolates in a sample. As the ANI value among the two sequenced genomes was very high (99.96%) but not identical, it is always possible that the residual 0.04% would be responsible for the differences of APPs by some unknown mechanism. Nonetheless, the *luxI* sequences, coding for the AHL synthase, as well as other putative *N*- acetyltransferases sequences are identical.

While it appears that we have different APPs belonging to a single genotype, the temporal sampling of *Vibrio* isolates in parallel to physicochemical parameters measurements allowed us to evaluate the variation in the "environment" leading to the phenotypic plasticity of AHL production. However, as the sampling was originally designed to evaluate the diversity of total *Vibrio* spp. (and not just that of *V. mediterranei* G1) the total numbers of evaluated strains are limited, and thus in the following discussion we point to major trends and propose ideas to be tested by more targeted studies.

Based on our DistLM analysis, phosphates concentration appeared as the most explanatory variable by being correlated with high abundances of non AHL producers. That was particularly striking on 21 June 2016, where the near totality of the strains belonged to the ($F117^-/MT102^-$) phenotype which coincided with a peak of phosphates likely associated with sediment resuspension. In order to explain this potential link between non-AHL producers and high phosphates concentrations, we propose a possible implication of the polyphosphate kinase activity. The whole genome analysis of the G1 isolates revealed few copies of the *ppk* gene and several studies have demonstrated that polyphosphate kinase (ppk) enhance the ability of bacteria to survive under environmental stresses. Since this enzyme has a negative impact on AHLs production in *P. fluorescens* and is repressed at high phosphates concentrations (Rashid *et al.,* 2000; Jahid *et al.,* 2006; Silby *et al.,* 2009), it is tempting to link the lack of AHL production to a repression of ppk by phosphates. As the peak of non AHL producers, the 2016/06/21, occurred at the highest phosphates concentration in the two years sampling, we hypothesized that in this context there is low expression of *ppk* gene and down regulation of AHL production (Rashid *et al.,* 2000).

The Salses-Leucate lagoon was also characterized by high *Cyanobacteria* concentrations, mainly *Synechococcus* species, ranging between 3.86×10^5 to 2.88×10^8 cells/L, making them an important part of the microbial community. Over the study, *Cyanobacteria* counts were highly correlated to the ($FF17^+/MT102^+$) phenotype abundances (Pearson correlation 77.3%; *p value* = 0.002; June/July 2015) but also to the peak of the ($F117^+/MT102^-$) phenotype (July 2016, **Figure 4**). In the past, *Vibrio* species have been associated to cyanobacterial blooms (Berg *et al.,* 2009), especially by benefiting from their derived organic matter (Eiler *et al.,* 2007). Mutual interactions were described between *Synechococcus* species and heterotrophic bacteria (Hayashi *et al.,* 2011), and co-culture experiments between *Vibrio* species and *Synechococcus* revealed a deleterious effect on the

cyanobacteria physiology especially on iron, phosphates and nitrogen pathways (Tai *et al.,* 2009). In the other hand, since *Synechococcus* species harbors "orphan" *luxR* genes, possibly encoding for the receptor LuxR involved in AHL signal reception, and shows quorum quenching activity against *Vibrio* species, complex QS-based relationships might occur between these two genera (Yoshino *et al.,* 2013; Honda *et al.,* 2014; Marsan *et al.,* 2014; Santhakumari *et al.,* 2016; Shimura *et al.,* 2017). Thereby, the temporal dynamic of different APPs can be related to changes in the cyanobacterial assemblages, switching between commensal/consumers, probably benefitting from cyanobacterial dissolved organic matter and competitors for inorganic nutrient such as phosphates, nitrogen and iron. Understanding the *in situ* interactions between APPs of *V. mediterranei* and cyanobacterial assemblages remains an interesting subject for future studies.

Overall, our results indicate a phenotypic plasticity of AHL production among isolates of a single genotype and converges towards the fact that our strains are harboring a single AHL synthase gene (*luxI*). The underlying physiological mechanisms leading to this phenotypic plasticity still yet to describe. However, it is well known that AHL synthases are catalyzing the reaction between S-adenosylmethionine (SAM) and acyl-ACPs to produce AHLs (Keller and Surette, 2006) and that the available acyl-ACP pools in bacteria may be susceptible to metabolic changes (Gould *et al*., 2005). Considering that it has been recognized that AHL production can be altered though the modulation of the fatty acid metabolic pathway and that the variation of APPs was explained at 83.4% by the environmental variables, it seems likely that fluctuations in the environment can change the nature of the produced AHLs (Hoang *et al.,* 2002; Gould *et al.,* 2006). However, the facts that 1) a near totality of the isolates were non-AHL producers at a time point and AHL-producers in a subsequent time point, and 2) that these phenotypes were observed after two rounds of isolation on rich medium, raises the intriguing possibility that epigenetic regulation might be

at play. It is well-known that the regulation of phenotypic variation is not always linked to changes in DNA sequence and can be epigenetic in nature (Smits *et al.,* 2006) and interestingly, Kurz *et al.* (2013) have shown that epigenetic mechanisms can be involved in the regulation of AHL-based QS system. We hypothesize that *V. mediterranei* strains could keep a memory of the social traits expressed in the environment. However, as any previous work have been published on the QS mechanisms of *V. mediterranei*, a consequent work on the description of the QS pathways and QS associated phenotypes still need to be achieved to confirm or deny this possible epigenetic control. Regardless of the mechanisms leading to the observed phenotypic variation, phenotypic plasticity should confer an increased fitness as heterogeneous populations should be better to adapt to rapid changes in the environment (Feinberg *et al*., 2010). The fact that the studied phenotypically plastic *V. mediterranei* populations thrive in a shallow lagoon subject to a relatively fast variation in physical and biogeochemical conditions supports this idea. Understanding the possible mechanisms of regulation of AHL-based QS in *V. mediterranei* remains a fascinating avenue for further studies.

Finally, our work highlight the phenotypic plasticity of AHL production among environmental *Vibrio* isolates. These results were obtained on strains after isolation and culture on rich media which underlines the fact that *Vibrio* isolates could retain a memory of *in situ* AHL production status. Considering the fact that quantification of AHL synthases expression by RTqPCR is still difficult due to a very low sequence homology among vibrios (Tait *et al*., 2010), the study of AHL-meditated QS by a biosensors based approach seems an interesting alternative to estimate whether or not AHL synthesis occurred in the environment.

Conclusion

382 QS is a well-studied social trait among *Vibrio* species, however, despite the current
383 knowledge obtained by *in vitro* studies on few species, there is a lack of studies regarding QS
384 in complex ecological communities. Our study provides a first investigation on the seasonal
385 dynamic of AHL producing *Vibrio* in a changing coastal environment and open new
386 perspectives for outgoing studies regarding QS mechanisms in natural habitats and a possible
387 epigenetic regulation of QS phenotypic plasticity.

388 ## Acknowledgements

389 We would like to thank Professor Marti Anderson for her support with all statistical
390 analyses using PRIMER 7. We are thankful to Christophe Canal for the sampling campaigns
391 at Leucate Lagoon, and for the physico-chemical analysis performed on water samples. We
392 also thanks Jocelyne Caparros for inorganic nutrient analysis and Nicole Batailler for her
393 technical assistance in some steps of the experimental work. Finally, we thank the Bio2Mar
394 platform for providing access to the analytical chemistry and molecular biology equipment.
395 We would like to thank Laurence Fonbonne from the "Syndicat RIVAGE" for her help and
396 for giving us the access to the lagoon. This work was supported by a Ph.D. grant from
397 doctoral school ED227 Sciences de la Nature et de l'Homme : évolution et écologie
398 associating Sorbonne Université and Museum National d'Histoire Naturelle (MNHN), France.

399

400 ## References

401 Agrawal, A.A., 2001. Phenotypic plasticity in the interactions and evolution of species.
402 *Science* **294**: 321–326.

403 Al-Bairuty, G.A., Shaw, B.J., Handy, R.D., Henry, T.B., 2013. Histopathological effects of
404 waterborne copper nanoparticles and copper sulphate on the organs of rainbow trout
405 (Oncorhynchus mykiss). *Aquat. Toxicol*. **126**: 104–115.

406 Anderson, Marti J, 2001. Permutation tests for univariate or multivariate analysis of variance
407 and regression. *Can. J. Fish. Aquat. Sci*. **58**: 626–639.

408 Anderson, Marti J., 2001. A new method for non-parametric multivariate analysis of variance:
409 non-parametric MANOVA for ecology. *Austral Ecol.* **26**: 32–46.

410 Aryal, D.R., Geissen, V., Ponce-Mendoza, A., Ramos-Reyes, R.R., Becker, M., 2012. Water
411 quality under intensive banana production and extensive pastureland in tropical Mexico. *J.*
412 *Plant Nutr. Soil Sci.* **175**: 553–559.

413 Ayrapetyan, M., Williams, T.C., Oliver, J.D., 2014. Interspecific Quorum sensing mediates
414 the resuscitation of viable but nonculturable vibrios. *Appl. Environ. Microbiol.* **80**: 2478–
415 2483.

416 Aziz, R.K., Bartels, D., Best, A.A., DeJongh, M., Disz, T., Edwards, R.A., Formsma, K., *et*
417 *al.,* 2008. The RAST Server: Rapid annotations using subsystems technology. *BMC*
418 *Genomics* **9**: 75.

419 Bari, S.M.N., Roky, M.K., Mohiuddin, M., Kamruzzaman, M., Mekalanos, J.J., Faruque,
420 S.M., 2013. Quorum-sensing autoinducers resuscitate dormant *Vibrio cholerae* in
421 environmental water samples. *Proc. Natl. Acad. Sci.* **110**: 9926–9931.

422 Bassler, B.L., Losick, R., 2006. Bacterially Speaking. *Cell* **125**: 237–246.

423 Bassler, B.L., Wright, M., Silverman, M.R., 1994. Multiple signalling systems controlling
424 expression of luminescence in *Vibrio harveyi*: sequence and function of genes encoding a
425 second sensory pathway. *Mol. Microbiol.* **13**: 273–286.

426 Ben-Haim, Y., 2003. *Vibrio coralliilyticus* sp. nov., a temperature-dependent pathogen of the
427 coral *Pocillopora damicornis*. *Int. J. Syst. Evol. Microbiol.* **53**: 309–315.

428 Berg, K.A., Lyra, C., Sivonen, K., Paulin, L., Suomalainen, S., Tuomi, P., *et al.,* 2009. High
429 diversity of cultivable heterotrophic bacteria in association with cyanobacterial water blooms.
430 *ISME J*. **3**: 314–325.

431 Bondí, R., Messina, M., De Fino, I., Bragonzi, A., Rampioni, G., Leoni, L., 2014. Affecting
432 *Pseudomonas aeruginosa* phenotypic plasticity by Quorum sensing dysregulation hampers
433 pathogenicity in murine chronic lung infection. *PLoS ONE* **9**: e112105.

434 Buchholtz, C., Nielsen, K.F., Milton, D.L., Larsen, J.L., Gram, L., 2006. Profiling of acylated
435 homoserine lactones of *Vibrio anguillarum in vitro* and *in vivo*: Influence of growth
436 conditions and serotype. *Syst. Appl. Microbiol.* **29**: 433–445.

437 Caraux, G., Pinloche, S., 2005. PermutMatrix: a graphical environment to arrange gene
438 expression profiles in optimal linear order. *Bioinformatics* **21**: 1280–1281.

439 Casadesus, J., Low, D., 2006. Epigenetic gene regulation in the bacterial world. *Microbiol.*
440 *Mol. Biol. Rev.* **70**: 830–856.

441 Chevin, L.-M., Lande, R., Mace, G.M., 2010. Adaptation, plasticity, and extinction in a
442 changing environment: Towards a predictive theory. *PLoS Biol.* **8**: e1000357.

443 Chimetto Tonon, L.A., Silva, B.S. de O., Moreira, A.P.B., Valle, C., Alves, N., Cavalcanti,
444 G., *et al.,* 2015. Diversity and ecological structure of vibrios in benthic and pelagic habitats
445 along a latitudinal gradient in the Southwest Atlantic Ocean. *PeerJ* **3**: e741.

446 Chong, G., Kimyon, Ö., Manefield, M., 2013. Quorum sensing signal synthesis may represent
447 a selective advantage independent of its role in regulation of bioluminescence in *Vibrio*
448 *fischeri. PLoS ONE* **8**: e67443.

449 Doberva, M., Sanchez-Ferandin, S., Ferandin, Y., Intertaglia, L., Joux, F., Lebaron, P., *et al.,*
450 2014. Genome sequence of *Maribius* sp. strain MOLA 401, a marine *Roseobacter* with a
451 Quorum-sensing cell-dependent physiology. *Genome Announc.* **2**: e00997-14-e00997-14.

452 Eiler, A., Gonzalez-Rey, C., Allen, S., Bertilsson, S., 2007. Growth response of *Vibrio*
453 *cholerae* and other *Vibrio* spp. to cyanobacterial dissolved organic matter and temperature in
454 brackish water: Cyanobacterial DOM, temperature and *Vibrio* growth. *FEMS Microbiol. Ecol.*
455 **60**: 411–418.

456 Feinberg, Andrew P., and Rafael A. Irizarry. "Stochastic epigenetic variation as a driving
457 force of development, evolutionary adaptation, and disease." *Proceedings of the National*
458 *Academy of Science*s 107.suppl 1 (2010): 1757-1764.

459 Fuqua, W.C., Winans, S.C., Greenberg, E.P., 1994. Quorum sensing in bacteria: the LuxR-
460 LuxI family of cell density-responsive transcriptional regulators. *J. Bacteriol.* **176**: 269–275.

461 García-Aljaro, C., Vargas-Cespedes, G.J., Blanch, A.R., 2012. Detection of acylated
462 homoserine lactones produced by *Vibrio* spp. and related species isolated from water and
463 aquatic organisms. *J. Appl. Microbiol.* **112**: 383–389.

464 Girard, L., Blanchet, E., Intertaglia, L., Baudart, J., Stien, D., Suzuki, *et al.,* 2017.
465 Characterization of N-acyl homoserine lactones in *Vibrio tasmaniensis* LGP32 by a
466 biosensor-based UHPLC-HRMS/MS Method. *Sensors* **17**: 906.

467 Goo, E., An, J.H., Kang, Y., Hwang, I., 2015. Control of bacterial metabolism by quorum
468 sensing. *Trends Microbiol.* **23**: 567–576.

469 Gould, T.A., Herman, J., Krank, J., Murphy, R.C., Churchill, M.E.A., 2006. Specificity of
470 acyl-homoserine lactone synthases examined by mass spectrometry. *J. Bacteriol.* **188**: 773–
471 783.

472 Ha, C., Kim, S.-K., Lee, M.-N., Lee, J.-H., 2014. Quorum sensing-dependent metalloprotease
473 VvpE is important in the virulence of *Vibrio vulnificus* to invertebrates. *Microb. Pathog.* 7**1–**
474 **72**: 8–14.

475 Hammer, B.K., Bassler, B.L., 2003. Quorum sensing controls biofilm formation in *Vibrio*
476 *cholerae. Mol. Microbiol.* **50**: 101–104.

477 Hayashi, S., Itoh, K., Suyama, K., 2011. Growth of the cyanobacterium *Synechococcus*
478 *leopoliensis* CCAP1405/1 on agar media in the presence of heterotrophic bacteria. *Microbes*
479 *Environ*. **26**: 120–127.

480 Heidelberg, J.F., Heidelberg, K.B., Colwell, R.R., 2002. Bacteria of the γ-subclass
481 proteobacteria associated with zooplankton in Chesapeake bay. *Appl. Environ. Microbiol.* **68**:
482 5498–5507.

483 Heras, J., Domínguez, C., Mata, E., Pascual, V., Lozano, C., Torres, C., *et al.,* 2015. GelJ – a
484 tool for analyzing DNA fingerprint gel images. *BMC Bioinformatics* **16**.

485 Hoang, T.T., Sullivan, S.A., Cusick, J.K., Schweizer, H.P., 2002. Beta-ketoacyl acyl carrier
486 protein reductase (FabG) activity of the fatty acid biosynthetic pathway is a determining
487 factor of 3-oxo-homoserine lactone acyl chain lengths. *Microbiol. Read. Engl.* **148**: 3849–
488 3856.

489 Honda, T., Liang, Y., Arai, D., Ito, Y., Yoshino, T., Tanaka, T., 2014. Draft genome sequence
490 of marine cyanobacterium *Synechococcus* sp. strain NKBG042902, which harbors a
491 homogeneous plasmid available for metabolic engineering. *Genome Announc.* **2**: e00704-14-
492 e00704-14.

493 Huang, Y.-L., Ki, J.-S., Lee, O.O., Qian, P.-Y., 2009. Evidence for the dynamics of acyl
494 homoserine lactone and AHL-producing bacteria during subtidal biofilm formation. *ISME J.*
495 **3**: 296–304.

496 Hulton, C.S., Higgins, C.F., Sharp, P.M., 1991. ERIC sequences: a novel family of repetitive
497 elements in the genomes of *Escherichia coli*, *Salmonella typhimurium* and other
498 enterobacteria. *Mol. Microbiol.* **5**: 825–834.

499 Jahid, I.K., Silva, A.J., Benitez, J.A., 2006. Polyphosphate stores enhance the ability of *Vibrio*
500 *cholerae* to overcome environmental stresses in a low-phosphate environment. *Appl. Environ.*
501 *Microbiol.* **72**: 7043–7049.

502 Joelsson, A., Liu, Z., Zhu, J., 2006. Genetic and phenotypic diversity of Quorum-sensing
503 systems in clinical and environmental isolates of *Vibrio cholerae. Infect. Immun.* **74**: 1141–
504 1147.

505 Karlson, B., Cusack, C., Bresnan, E., 2010. Microscopic and molecular methods for
506 quantitative phytoplankton analysis.

507 Keller, L., Surette, M.G., 2006. Communication in bacteria: an ecological and evolutionary
508 perspective. *Nat. Rev. Microbiol.* **4**: 249–258.

509 Khan, A.A., McCarthy, S., Wang, R.-F., Cerniglia, C.E., 2002. Characterization of United
510 States outbreak isolates of *Vibrio parahaemolyticus* using enterobacterial repetitive intergenic
511 consensus (ERIC) PCR and development of a rapid PCR method for detection of O3: K6
512 isolates. *FEMS Microbiol. Lett.* **206**: 209–214.

513 Kurz, V., Nelson, E.M., Perry, N., Timp, W., Timp, G., 2013. Epigenetic memory emerging
514 from integrated transcription bursts. *Biophys. J.* **105**: 1526–1532.

515 Le Roux, F., Gay, M., Lambert, C., Nicolas, J.-L., Gouy, M., Berthe, F.C.J., 2004.
516 Phylogenetic study and identification of *Vibrio splendidus*-related strains based on *gyrB* gene
517 sequences. *Dis. Aquat. Organ.* **58**: 143.

518 Lennon, J.T., Jones, S.E., 2011. Microbial seed banks: the ecological and evolutionary
519 implications of dormancy. *Nat. Rev. Microbiol.* **9**: 119–130.

520 Li, L., Mendis, N., Trigui, H., Oliver, J.D., Faucher, S.P., 2014. The importance of the viable
521 but non-culturable state in human bacterial pathogens. *Front. Microbiol.* **5**.

522 Lorenzen, C.J., 1967. Determination of cholophyll and pheo-pigments: spectrophotometric
523 equations. *Limnol. Oceanogr.* **12**: 343–346.

524 Lorenzen, C.J., 1966. A method for the continuous measurement of in vivo chlorophyll
525 concentration. *Deep Sea Res. Oceanogr. Abstr.* **13**: 223–227.

526 Marie, D., Rigaut-Jalabert, F., Vaulot, D., 2014. An improved protocol for flow cytometry
527 analysis of phytoplankton cultures and natural samples: An improved protocol for flow
528 cytometry analysis. *Cytometry A* **85**: 962–968.

529 Marsan, D., Wommack, K.E., Ravel, J., Chen, F., 2014. Draft genome sequence of
530 *Synechococcus* sp. strain CB0101, isolated from the chesapeake bay estuary. *Genome*
531 *Announc.* ***2***: e01111-13-e01111-13.

532 McArdle, B.H., Anderson, M.J., 2001. Fitting multivariate models to community data: A
533 comment on distance-based redundancy analysis. *Ecology* **82**: 290.

534 Natrah, F.M.I., Ruwandeepika, H.A.D., Pawar, S., Karunasagar, I., Sorgeloos, P., Bossier, P.,
535 *et al.,* 2011. Regulation of virulence factors by quorum sensing in *Vibrio harveyi. Vet.*
536 *Microbiol.* **154**: 124–129.

537 Olm, M.R., Brown, C.T., Brooks, B., Firek, B., Baker, R., Burstein, D., *et al.,* 2017. Identical
538 bacterial populations colonize premature infant gut, skin, and oral microbiomes and exhibit
539 different in situ growth rates. *Genome Res.* gr.213256.116.

540 Persat, A., Nadell, C.D., Kim, M.K., Ingremeau, F., Siryaporn, A., Drescher, *et al.,* 2015. The
541 mechanical world of bacteria. *Cell* **161**: 988–997.

542 Pfeffer, C., Oliver, J.D., 2003. A comparison of thiosulphate-citrate-bile salts-sucrose (TCBS)
543 agar and thiosulphate-chloride-iodide (TCI) agar for the isolation of *Vibrio* species from
544 estuarine environments. *Lett. Appl. Microbiol*. **36**: 150–151.

545 Platt, T.G., Fuqua, C., 2010. What's in a name? The semantics of quorum sensing. *Trends*
546 *Microbiol.* **18**: 383–387.

547 Purohit, A.A., Johansen, J.A., Hansen, H., Leiros, H.-K.S., Kashulin, A., Karlsen, *et al.,* 2013.
548 Presence of acyl-homoserine lactones in 57 members of the *Vibrionaceae* family. *J. Appl.*
549 *Microbiol.* **115**: 835–847.

Rashid, M.H., Rumbaugh, K., Passador, L., Davies, D.G., Hamood, A.N., Iglewski, B.H., *et al.,* 2000. Polyphosphate kinase is essential for biofilm development, quorum sensing, and virulence of *Pseudomonas aeruginosa. Proc. Natl. Acad. Sci.* **97**: 9636–9641.

Rasmussen, B., Nielsen, K., Machado, H., Melchiorsen, J., Gram, L., Sonnenschein, E., 2014. Global and phylogenetic distribution of Quorum sensing signals, acyl homoserine lactones, in the family of *Vibrionaceae. Mar. Drugs* **12**: 5527–5546.

Rembauville, M., Blain, S., Caparros, J., Salter, I., 2016. Particulate matter stoichiometry driven by microplankton community structure in summer in the Indian sector of the Southern Ocean: Particulate matter stoichiometry. *Limnol. Oceanogr.* **61**: 1301–1321.

Rivera, I.G., Chowdhury, M.A., Huq, A., Jacobs, D., Martins, M.T., Colwell, R.R., 1995. Enterobacterial repetitive intergenic consensus sequences and the PCR to generate fingerprints of genomic DNAs from *Vibrio cholerae* O1, O139, and non-O1 strains. *Appl. Environ. Microbiol.* **61**: 2898–2904.

Romero, E., Peters, F., Guadayol, Ò., 2013. The interplay between short-term, mild physicochemical forcing and plankton dynamics in a coastal area. *Limnol. Oceanogr.* **58**: 903–920.

Santhakumari, S., Kannappan, A., Pandian, S.K., Thajuddin, N., Rajendran, R.B., Ravi, A.V., 2016. Inhibitory effect of marine cyanobacterial extract on biofilm formation and virulence factor production of bacterial pathogens causing vibriosis in aquaculture. *J. Appl. Phycol.* **28**: 313–324.

Schwartzman, J.A., Ruby, E.G., 2015. A conserved chemical dialog of mutualism: lessons from squid and vibrio. *Microbes Infect.*

572 Shimura, Y., Hirose, Y., Misawa, N., Wakazuki, S., Fujisawa, T., Nakamura, *et al.,* 2017.
573 Complete genome sequence of a coastal cyanobacterium, *Synechococcus* sp. strain NIES-970.
574 *Genome Announc.* **5**: e00139-17.

575 Silby, M.W., Nicoll, J.S., Levy, S.B., 2009. Requirement of polyphosphate by *Pseudomonas*
576 *fluorescens* Pf0-1 for competitive fitness and heat tolerance in laboratory media and sterile
577 *Soil. Appl. Environ. Microbiol.* **75**: 3872–3881.

578 Smits, W.K., Kuipers, O.P., Veening, J.-W., 2006. Phenotypic variation in bacteria: the role
579 of feedback regulation. *Nat. Rev. Microbiol.* **4**: 259–271.

580 Snitkin, E.S., Zelazny, A.M., Thomas, P.J., Stock, F., NISC Comparative sequencing program
581 group, Henderson, D.K., Palmore, T.N., Segre, J.A., 2012. Tracking a hospital outbreak of
582 carbapenem-resistant *Klebsiella pneumoniae* with whole-genome sequencing. *Sci. Transl.*
583 *Med.* **4**: 148ra116.

584 Soto, W., Gutierrez, J., Remmenga, M.D., Nishiguchi, M.K., 2009. Salinity and temperature
585 effects on physiological responses of *Vibrio fischeri* from diverse ecological niches. *Microb.*
586 *Ecol.* **57**: 140–150.

587 Tai, V., Paulsen, I.T., Phillippy, K., Johnson, D.A., Palenik, B., 2009. Whole-genome
588 microarray analyses of *Synechococcus* - *Vibrio* interactions. *Environ. Microbiol*. **11**: 2698–
589 2709.

590 Tait, K., Hutchison, Z., Thompson, F.L., Munn, C.B., 2010. Quorum sensing signal
591 production and inhibition by coral-associated vibrios. *Environ. Microbiol. Rep.* **2**: 145–150.

592 Takemura, A.F., Chien, D.M., Polz, M.F., 2014. Associations and dynamics of *Vibrionaceae*
593 in the environment, from the genus to the population level. *Front. Microbiol.* **5**.

Vezzulli, L., Pezzati, E., Stauder, M., Stagnaro, L., Venier, P., Pruzzo, C., 2015. Aquatic ecology of the oyster pathogens *Vibrio splendidus* and *Vibrio aestuarianus*. *Environ. Microbiol.* **17**: 1065–1080.

Vouvé, F., Buscail, R., Aubert, D., Labadie, P., Chevreuil, M., Canal, *et al.,* 2014. Bages-Sigean and Canet-St Nazaire lagoons (France): physico-chemical characteristics and contaminant concentrations (Cu, Cd, PCBs and PBDEs) as environmental quality of water and sediment. *Environ. Sci. Pollut. Res.* **21**: 3005–3020.

Wagner-Döbler, I., Thiel, V., Eberl, L., Allgaier, M., Bodor, A., Meyer, *et al.,* 2005. Discovery of complex mixtures of novel long-chain Quorum sensing signals in free-living and host-associated marine *Alphaproteobacteria. ChemBioChem* **6**: 2195–2206.

Watson, W.T., Minogue, T.D., Val, D.L., Von Bodman, S.B., Churchill, M.E.A., 2002. Structural basis and specificity of acyl-homoserine lactone signal production in bacterial Quorum sensing. *Mol. Cell* **9**: 685–694.

Wendling, C.C., Wegner, K.M., 2015. Adaptation to enemy shifts: rapid resistance evolution to local *Vibrio* spp. in invasive Pacific oysters. *Proc. R. Soc. B Biol. Sci.* **282**: 20142244–20142244.

West, S.A., Diggle, S.P., Buckling, A., Gardner, A., Griffin, A.S., 2007. The social lives of microbes. *Annu. Rev. Ecol. Evol. Syst.* **38**: 53–77.

West, S.A., Griffin, A.S., Gardner, A., Diggle, S.P., 2006. Social evolution theory for microorganisms. *Nat. Rev. Microbiol.* **4**: 597–607.

West-Eberhard, M.J., 2003. Developmental plasticity and evolution. Oxford University Press, Oxford ; New York.

Whitesides, M.D., Oliver, J.D., 1997. Resuscitation of *Vibrio* vulnificus from the viable but nonculturable state. *Appl. Environ. Microbiol.* **63**: 1002–1005.

Yamamoto, S., Harayama, S., 1995. PCR amplification and direct sequencing of *gyrB* genes with universal primers and their application to the detection and taxonomic analysis of *Pseudomonas putida* strains. *Appl. Environ. Microbiol.* **61**: 1104–1109.

Yoshino, T., Honda, T., Tanaka, M., Tanaka, T., 2013. Draft genome sequence of marine cyanobacterium *Synechococcus* sp. Strain NKBG15041c. *Genome Announc.* **1**: e00954-13-e00954-13.

Zhu, J., Miller, M.B., Vance, R.E., Dziejman, M., Bassler, B.L., Mekalanos, J.J., 2002. Quorum-sensing regulators control virulence gene expression in *Vibrio cholerae. Proc. Natl. Acad. Sci.* **99**: 3129–3134.

Figure 1 Temporal dynamic of *V. mediterranei* isolates relative to all *Vibrio* spp. isolates. **A**. G1-G22 are Genotypes based on ERIC-PCR; **B**. APP: AHL Production Phenotypes; where F117+ and F117- are isolates detectable or not by the biosensor *Pseudomonas putida* (pKR-C12) and MT102+ and MT102- are detectable or not by the biosensor *Escherichia coli* (pJBA-132).

Figure 2 Heat-Map of AHL diversity in *V. mediterranei* G1 isolates by UHPLC-HRMS/MS (Ward's classification based on Jaccard index; Caraux and Pinloche, 2005). **1**: 17LN0615E and **2**: 2LS0615E corresponding to the $F117^{+}/MT102^{+}$ phenotype; **3**: 21LN0615E and **4**: 9LS0615E corresponding to the $F117^{+}/MT102^{-}$ phenotype. (*) unanticipated AHLs corresponding to any analyzed AHL standards. Grey squares represent the absence of AHL.

Figure 3 The dbRDA ordination representing the results of the DistLM analysis in 2D. The DistLM is used to examine the relationship between the distribution and temporal dynamics of *V. mediterranei* G1 APP and all measured environmental variables. Vectors represent predictor variables used for the construction of the constrained ordination (the dbRDA diagram), and the length of the vectors represents the explanatory percentage of each variable. The analysis is detailed **Table 2.**

Figure 4 Principal co-ordinate plot (PCO) of *V. mediterranei* G1 phenotypes for the first and second principal co-ordinates using the Bray-Curtis similarity matrix. Phytoplankton and Bacteria counts were used as predictor variables, are shown here only the variable with Pearson correlation >0.45. The analysis is detailed in **Supplementary Table 4** and the contribution of each variable in the construction of PCO axis (Pearson correlation) is detailed in **Supplementary Table 5**.

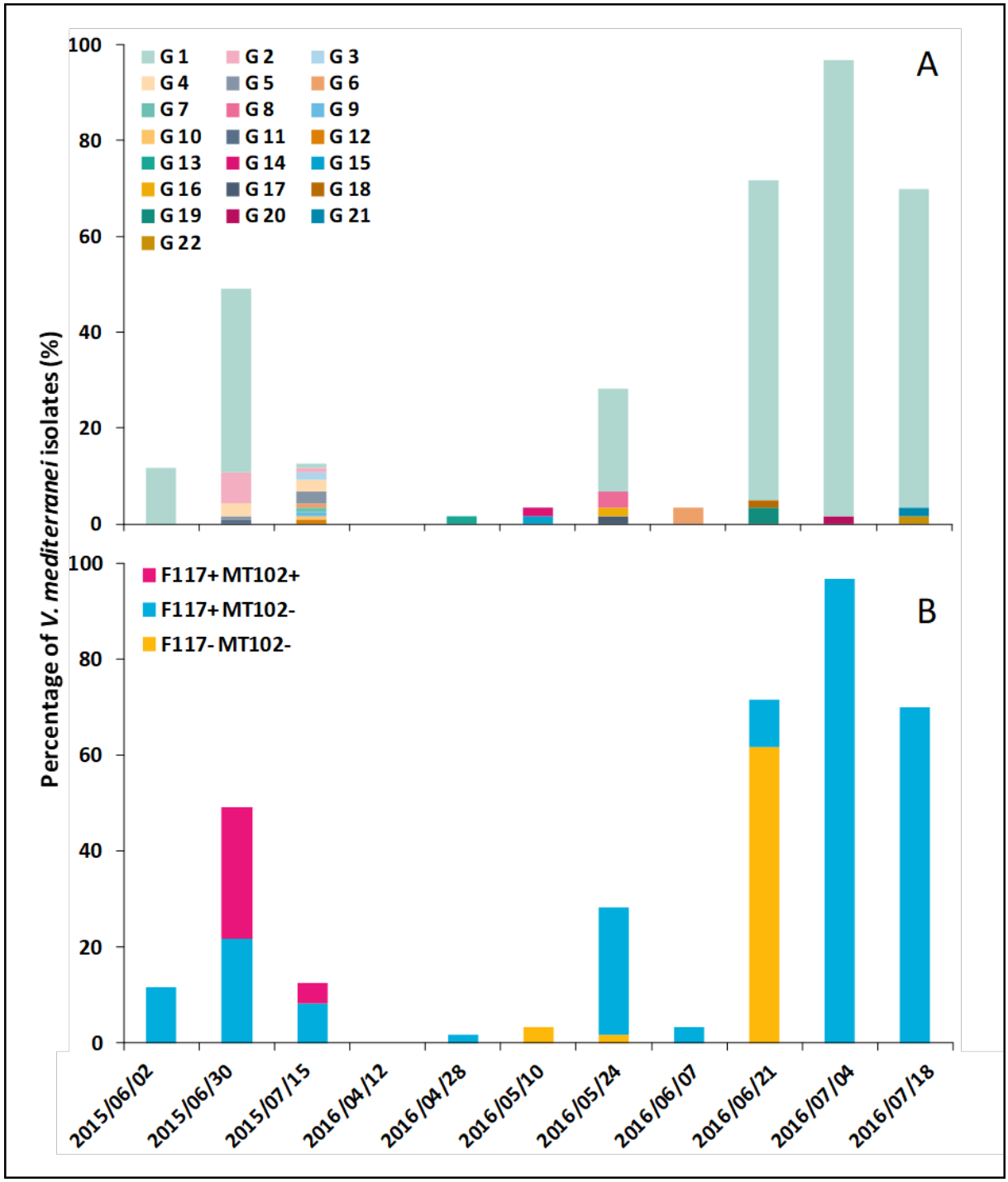
A
G 1
G 2
G 3
G 4
G 5
G 6
G 7
G 8
G 9
G 10
G 11
G 12
G 13
G 14
G 15
G 16
G 17
G 18
G 19
G 20
G 21
G 22
B
F117+ MT102+
F117+ MT102-
F117- MT102-
Percentage of V. mediterranei isolates (%)
100
80
60
40
20
0
2015/06/02
2015/06/30
2015/07/15
2016/04/12
2016/04/28
2016/05/10
2016/05/24
2016/06/07
2016/06/21
2016/07/04
2016/07/18

Figure 1

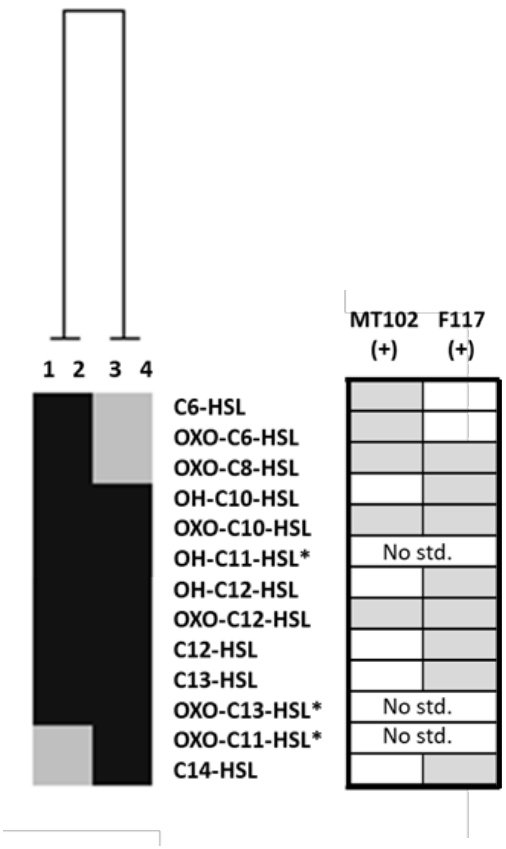
MT102 (+)
F117 (+)
1 2 3 4
C6-HSL
OXO-C6-HSL
OXO-C8-HSL
OH-C10-HSL
OXO-C10-HSL
OH-C11-HSL*
OH-C12-HSL
OXO-C12-HSL
C12-HSL
C13-HSL
OXO-C13-HSL*
OXO-C11-HSL*
C14-HSL
No std.
No std.
No std.

Figure 2

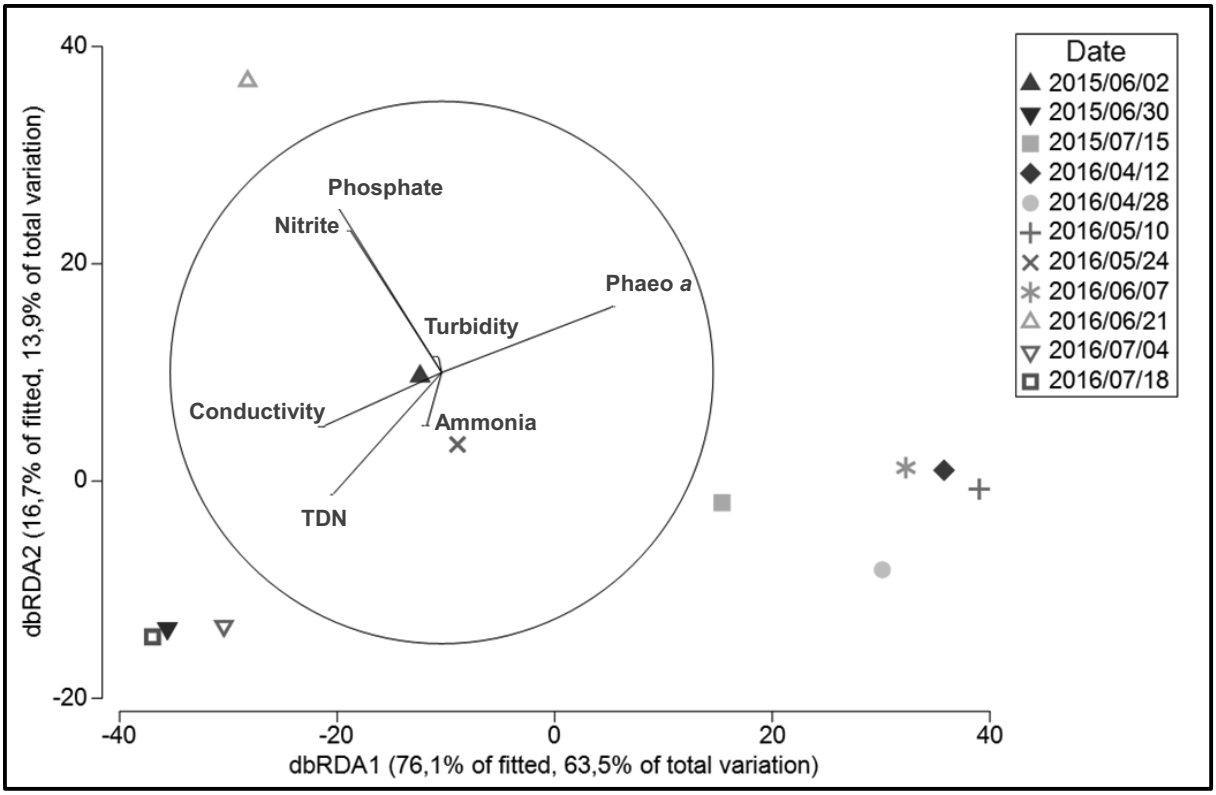
Date
2015/06/02
2015/06/30
2015/07/15
2016/04/12
2016/04/28
2016/05/10
2016/05/24
2016/06/07
2016/06/21
2016/07/04
2016/07/18
Phosphate
Nitrite
Phaeo a
Turbidity
Conductivity
Ammonia
TDN
40
20
0
-20
-40
-20
0
20
40
dbRDA2 (16,7% of fitted, 13,9% of total variation)
dbRDA1 (76,1% of fitted, 63,5% of total variation)

Figure 3.

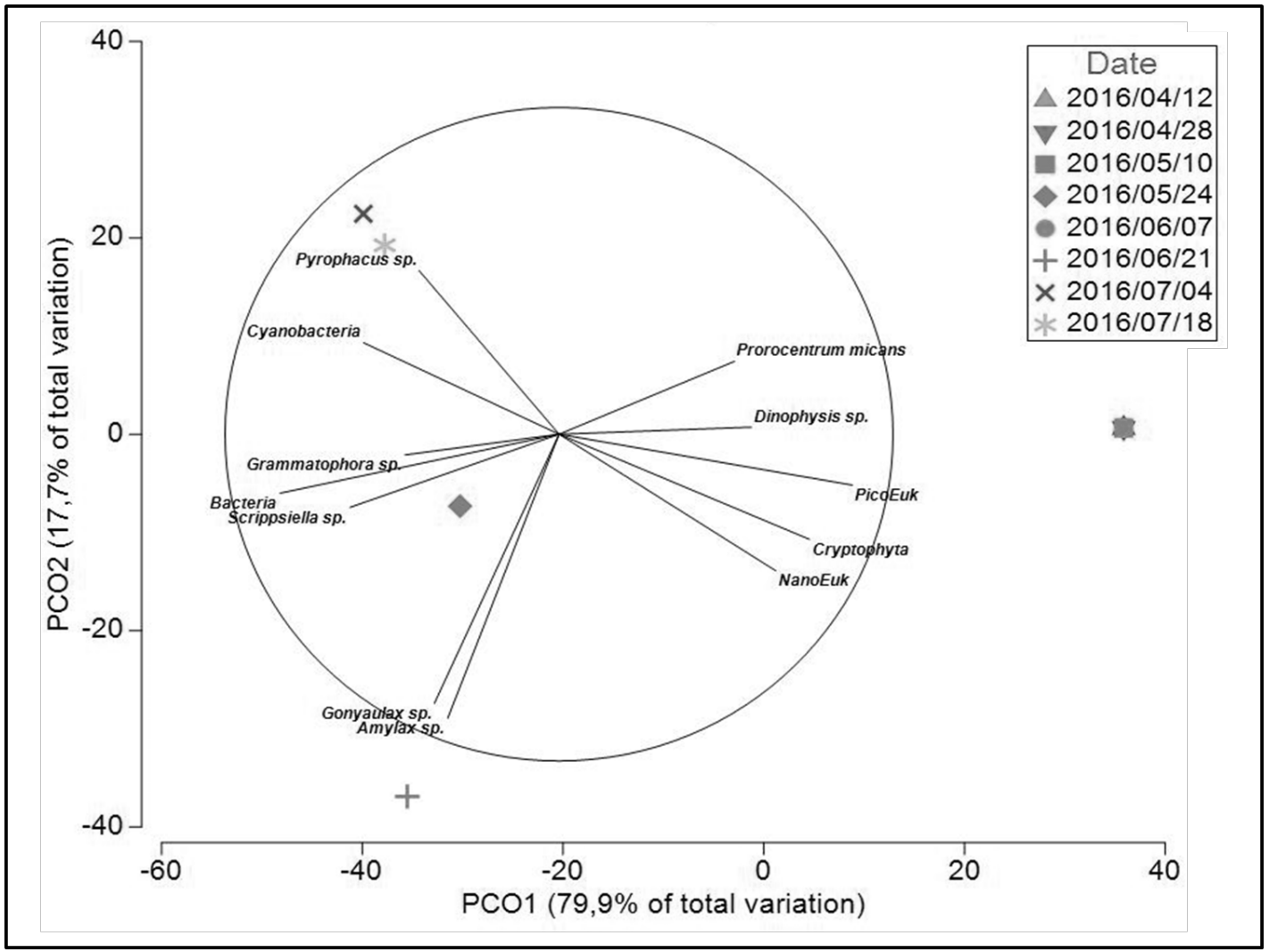
Date
2016/04/12
2016/04/28
2016/05/10
2016/05/24
2016/06/07
2016/06/21
2016/07/04
2016/07/18
Pyrophacus sp.
Cyanobacteria
Prorocentrum micans
Dinophysis sp.
Grammatophora sp.
Bacteria
Scrippsiella sp.
PicoEuk
Cryptophyta
NanoEuk
Gonyaulax sp.
Amylax sp.
PCO2 (17,7% of total variation)
PCO1 (79,9% of total variation)
40
20
0
-20
-40
-60
-40
-20
0
20
40

Figure 4.

Table 1 Environmental parameters measurements

Parameter	Methods/Instrumentation	Reference	Unit	Ranges	
				-	+
Temperature	Hach HQ40d multi	Al-Bairuty *et al.*, 2013; Vouvé *et al.*, 2014	° celcius	14.2	26.4
Salinity			‰	32.8	40.1
Conductivity			mS/cm	39.9	55.7
DO concentration			mg/L	7.82	10.09
DO saturation			%	91.7	116
pH			*	7.32	8.5
Nitrates	Hach DR/890 Colorimeter	Aryal *et al.*, 2012; Vouvé *et al.*, 2014	mg/L	1.89	9.26
Nitrites			mg/L	0.002	0.043
Ammonium			mg/L	<0.03	
Phosphates			mg/L	0.05	0.15
DOC	V_{CSN}/TNM-1 Shimadzu TOC/TN analyzer	Romero *et al.*, 2013; Vouvé *et al*., 2014	mg/L	2.5	6.69
TDN			mg/L	0.15	0.59
POC	Perkin Elmer C,H,N 2400	Rembauville *et al*., 2016	mg/L	217.635	453.27
PON			mg/L	36.99	92.40
Chlorophyll *a*	Lorenzen	Lorenzen, 1966; Lorenzen, 1967	µg/L	0.08	1.23
Phaeophytin *a*			µg/L	0.021	1.34
Cryptophyta	FACSCantoII	Marie *et al*., 2014	cells/L	6.74×10^2	1.65×10^6
Nanoeukaryote			cells/L	6.13×10^5	1.01×10^7
Picoeukaryote			cells/L	1.84×10^5	2.55×10^7
Cyanobacteria			cells/L	3.86×10^5	2.88×10^8
Bacteria			cells/L	3.04×10^9	2.14×10^{10}

Table 2: Test statistics for Distance-based Linear Model (DISTLM) analyses marginal and sequential tests based on 'Forward' procedure and AIC criteria of *V. mediterranei* G1 phenotypes abundance at the 11 sampling dates. Marginal tests show how much variation each variable explains when considered alone, ignoring other variables. Sequential tests explain the cumulative variation attributed to each variable fitted to the model in the order specified, taking previous variables into account.

Marginal Tests							
Variable	AIC	SS (trace)	Pseudo-*F*	P	Prop.	Cumul.	res.df
Phosphates	-	11291.0	11.953	0.002	0.3741	-	-
Conductivity	-	9146.6	8.696	0.002	0.3030	-	-
TDN	-	2788.2	2.035	0.137	0.0924	-	-
Nitrites	-	4424.8	3.435	0.039	0.1466	-	-
Phaeo *a*	-	8055.3	7.280	0.006	0.2669	-	-
Turbidity	-	1490.9	1.039	0.322	0.0494	-	-
Ammonia	-	2821.9	2.062	0.138	0.0935	-	-
Sequential tests							
+ Phosphates	152.62	11291.0	11.953	0.001	**0.3741**	0.3741	20
+ Conductivity	148.16	4810.1	6.490	0.008	**0.1594**	0.5335	19
+ TDN	145.80	2530.8	3.944	0.014	**0.0838**	0.6173	18
+ Nitrites	143.97	1846.0	3.234	0.057	**0.0612**	0.6785	17
+ Phaeo *a*	141.94	1624.1	3.216	0.052	**0.0538**	0.7323	16
+ Turbidity	138.66	1723.3	4.066	0.031	**0.0571**	0.7894	15
+ Ammonia	135.41	1350.8	3.777	0.032	**0.0448**	**0.8341**	14

SUPPLEMENTARY INFORMATION

Fig S1: Location of the sampling site within the Salses-Leucate Mediterranean lagoon.

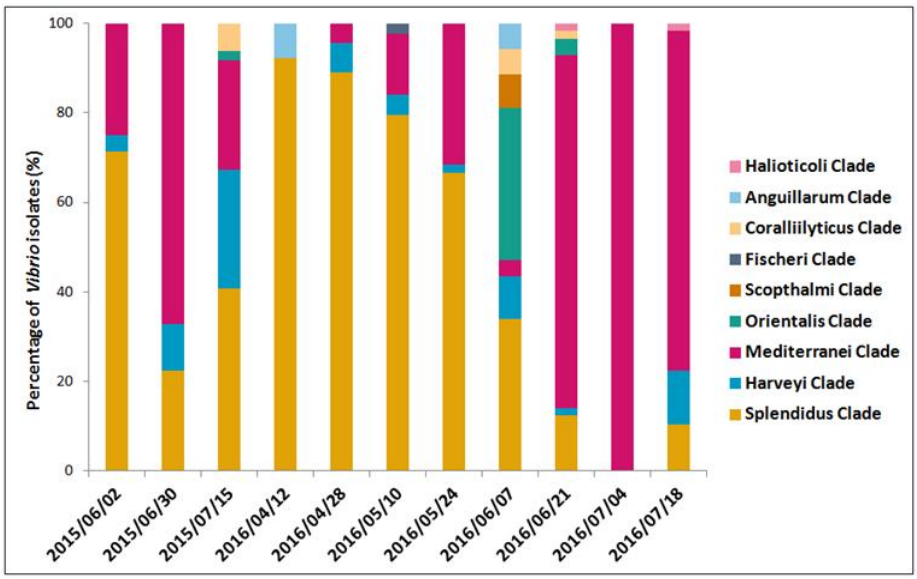

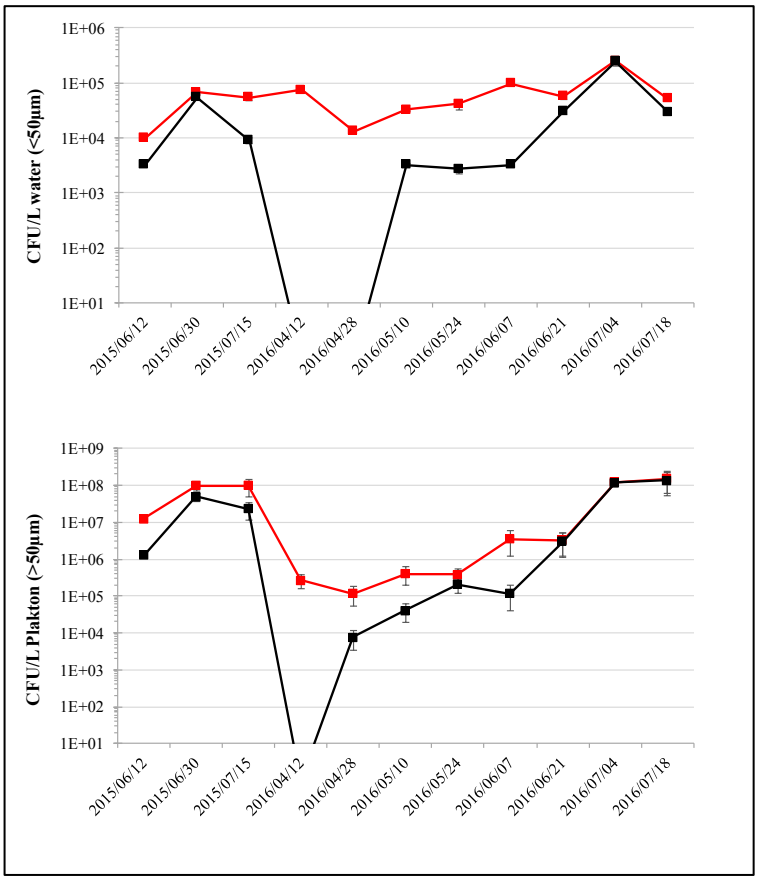

Fig S2: Temporal dynamic of *Vibrio* spp. isolates. (A). Relative proportion of isolates related – clade amongthe isolates identified as *Vibrio* spp. (B). Abundance in water and plankton of total culturable *Vibrio* spp. (red line) and culturable *V. mediterranei* (back line)

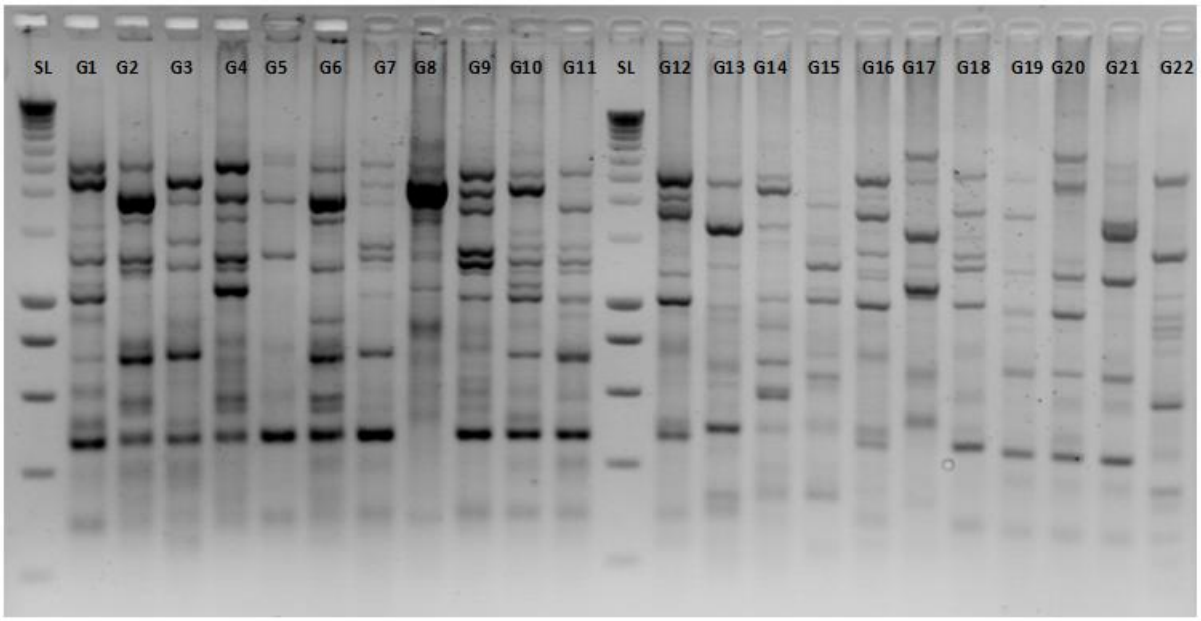

Fig S3: Agarose gel electrophoresis of *V. mediterranei* isolates using ERIC 1R and ERIC 2 primers.

SL: Smart Ladder marker, G1 to G22 : 22 Genotypes of *V. mediterranei*.

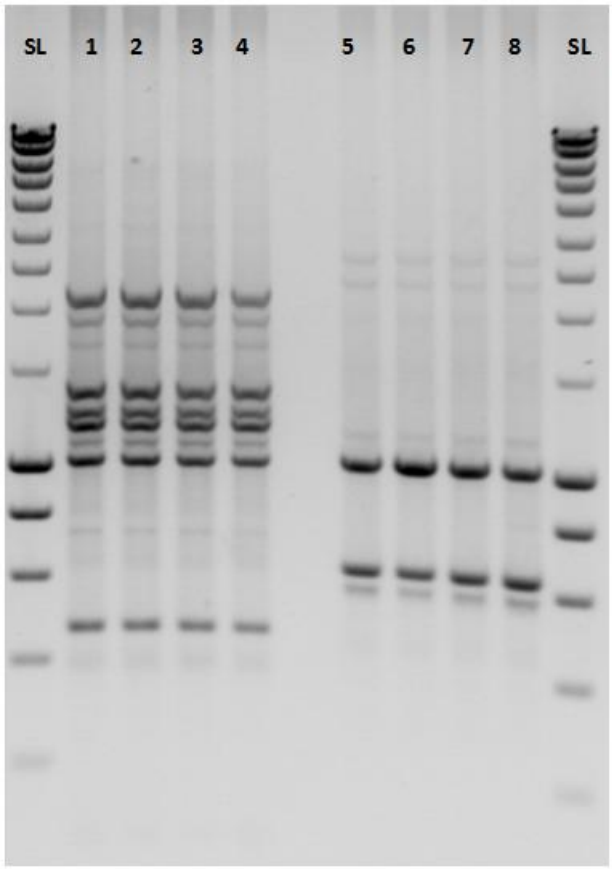

Fig S4: Agarose gel electrophoresis of Genotype 1 *V. mediterranei* isolates using: ERIC 1R and ERIC 2 (lanes 1-4); BOX A1R (5-8). **1, 5**: 2LS0615E; **2, 6**: 9LS0615E; **3, 7**: 17LN0615E; **4, 8**: 21LN0615E.

Table S1: Raw data table of *V. mediterranei* G1 phenotypes abundances.

	F117- MT102-	F117+ MT102-	F117+ MT102+	Fraction	Month	Year
2015/06/02 P	1	1	0	Particule associated	June	2015
2015/06/02 W	0	11	0	Water column	June	2015
2015/06/30 P	0	12	4	Particule associated	June	2015
2015/06/30 W	0	10	18	Water column	June	2015
2015/07/15 P	0	1	0	Particule associated	Jully	2015
2015/07/15 W	0	0	0	Water column	Jully	2015
2016/04/12 P	0	0	0	Particule associated	April	2016
2016/04/12 W	0	0	0	Water column	April	2016
2016/04/28 P	0	0	0	Particule associated	April	2016
2016/04/28 W	0	0	0	Water column	April	2016
2016/05/10 P	0	0	0	Particule associated	May	2016
2016/05/10 W	0	0	0	Water column	May	2016
2016/05/24 P	1	11	0	Particule associated	May	2016
2016/05/24 W	0	0	0	Water column	May	2016
2016/06/07 P	0	0	0	Particule associated	June	2016
2016/06/07 W	0	0	0	Water column	June	2016
2016/06/21 P	23	3	0	Particule asscoiated	June	2016
2016/06/21 W	11	4	0	Water column	June	2016
2016/07/04 P	0	28	0	Particule associated	Jully	2016
2016/07/04 W	0	29	0	Water column	Jully	2016
2016/07/18 P	0	27	0	Particule associated	Jully	2016
2016/07/18 W	0	13	0	Water column	Jully	2016

Table S2: Raw data table of environmental variables.

	2015/06/02	2015/06/30	2015/07/15	2016/04/12	2016/04/28	2016/05/10	2016/05/24	2016/06/07	2016/06/21	2016/07/04	2016/07/18
Temperature	17 .3	26 .4	24 .3	14 .6	14 .2	16	16 .9	22 .6	20 .8	23 .6	21 .5
Salinity	33 .6	35 .1	36 .7	32 .8	35 .6	36 .2	36 .3	35 .9	37 .1	38 .2	40 .1
Conductivity	48 .6	54 .2	54 .6	39 .9	42 .5	45 .2	46 .1	51 .4	50 .9	55 .4	55 .7
Dissolved oxygen	10 .09	8 .13	8 .11	9 .62	9 .96	9 .14	9 .02	9 .08	8 .22	7 .82	9 .13
pH	8 .5	8 .26	7 .5	7 .38	8 .41	8 .13	8 .22	8 .25	8 .25	8 .15	8 .29
Turbidity	1 .58	0 .68	1 .63	2 .45	3 .66	9 .21	7 .99	0 .98	4 .58	3 .54	1 .08
Nitrate	4 .26	3 .03	3 .65	9 .26	5 .53	1 .89	3 .47	3 .27	3 .69	3 .66	5 .15
Nitrite	0 .006	0 .007	0 .002	0 .014	0 .009	0 .003	0 .023	0 .011	**0 .043**	0 .023	0 .004
Ammonia	0 .03	0 .06	0 .05	0 .03	0 .03	0 .03	0 .03	0 .03	0 .03	0 .03	0 .03
Phosphate	**0 .12**	**0 .13**	0 .07	0 .07	0 .05	0 .07	0 .09	0 .05	**0 .15**	0 .06	0 .12
DOC	2 .74	2 .96	2 .54	2 .50	4 .72	4 .98	6 .12	6 .69	5 .27	5 .71	6 .66
TDN	0 .28	0 .55	0 .15	0 .47	0 .40	0 .43	0 .44	0 .27	0 .40	0 .33	0 .59
POC	319 .51	267 .98	217 .635	453 .27	305 .35	442 .95	372 .24	312 .55	297 .74	283 .30	237 .12
PON	49 .33	41 .56	36 .99	92 .40	59 .09	63 .79	56 .15	49 .84	43 .52	48 .17	41 .20
Chl a	0 .13	0 .082	0 .08	0 .72	0 .94	1 .08	1 .23	0 .76	0 .65	0 .39	0 .21
Phaeo a	0 .031	0 .024	0 .021	1 .13	1 .00	1 .34	0 .99	0 .59	0 .60	0 .36	0 .26

Table S3: Raw data table of phytoplankton and bacteria counts.

	2016/04/12	2016/04/28	2016/05/10	2016/05/24	2016/06/07	2016/06/21	2016/07/04	2016/07/18
Chaetoceros + Bacteriastrum sp.	0	800	80	0	83000	960	0	0
Coscinodiscus sp.	0	0	3600	0	0	160	0	200
Diploneis + Cocconeis sp.	0	320	1040	0	0	0	800	0
Grammatophora sp.	0	0	2720	5100	0	960	3800	0
Navicula and assimilated	352	2240	2960	19360	950	3400	12100	0
Nitzschia sp.	50	160	2560	22000	480	1760	160	0
Pseudo-Nitzschia sp.	0	0	0	2200	16000	1300	1800	0
Rhizosolenia sp.	0	0	80	0	0	0	0	0
Thalassionema nitzschïodes	100	0	0	0	0	0	0	0
Alexandrium sp.	580	480	80	100	320	640	160	640
Amylax sp.	0	0	0	100	160	1400	0	0
Ceratium sp.	0	0	0	1760	0	0	0	200
Dinophysis sp.	0	0	160	0	160	0	0	0
Gonyaulax sp.	0	0	0	0	0	160	0	0
Prorocentrum micans	140	1280	1520	0	2000	320	320	1000
Prorocentrum minimum	0	160	0	4300	41000	100	880	400
Protoperidinium sp.	0	0	0	0	1120	100	80	200
Pyrophacus sp.	0	0	0	0	0	0	480	0
Scrippsiella sp.	0	0	960	2900	2700	3000	1800	1600
Cryptophyta	7.56×10^5	1.65×10^6	4.73×10^5	8.61×10^5	1.05×10^6	1.87×10^5	9.37×10^2	2.81×10^3
NanoEuk	6.97×10^6	1.01×10^7	5.78×10^6	7.37×10^6	4.91×10^6	4.42×10^6	1.97×10^6	1.80×10^6
PicoEuk	1.66×10^7	2.35×10^7	1.53×10^7	4.95×10^6	6.40×10^6	2.22×10^6	9.58×10^5	1.84×10^5
Cyanobacteria	3.86×10^5	6.41×10^7	3.25×10^7	2.74×10^7	4.92×10^7	6.81×10^7	1.08×10^8	1.23×10^8
Bacteria	4.74×10^9	7.52×10^9	3.53×10^9	2.14×10^{10}	6.11×10^9	1.34×10^{10}	1.20×10^{10}	1.13×10^{10}

Table S4: PCO analysis, variation explained by individual axis.

Axis	Eigenvalue	Individual%	Cumulative%
PCO1	10339.0	79.9	79.9
PCO2	2291.7	17.7	97.6
PCO3	310.1	2.4	100.0
PCO4	6.6	0.1	100.0

Table S5: Pearson correlation between each variable and *V. mediterranei* G1 phenotypes ordination by axis.

Variable	PCO1	PCO2	PCO3	PCO4
Chaetoceros + Bacteriastrum sp.	0.3957	-0.0746	0.0727	-0.0074
Coscinodiscus sp.	0.2091	-0.0596	0.1201	-0.2093
Diploneis + Cocconeis sp.	0.1765	0.3734	0.2915	0.4676
Grammatophora sp.	**-0.4613**	-0.0634	-0.3167	0.6165
Navicula and assimilated	-0.4203	-0.1030	-0.4395	0.7537
Nitzschia sp.	-0.2447	-0.3751	-0.8087	0.2763
Pseudo-Nitzschia sp.	0.0122	-0.1159	-0.0715	0.2894
Rhizosolenia sp.	0.3770	0.0141	0.0226	-0.0003
Thalassionema nitzschïodes	0.3770	0.0141	0.0226	-0.0003
Alexandrium sp.	-0.0268	-0.2175	0.4391	-0.5969
Amylax sp.	-0.3331	**-0.8688**	0.1870	-0.0066
Ceratium sp.	-0.4481	-0.0184	-0.8920	-0.0565
Dinophysis sp.	**0.5759**	0.0215	0.0346	-0.0004
Gonyaulax sp.	-0.3734	**-0.8242**	0.4209	-0.0642
Prorocentrum micans	**0.5253**	0.2231	0.4144	-0.3464
Prorocentrum minimum	0.1879	0.0392	-0.2027	0.0875
Protoperidinium sp.	-0.0147	0.0849	0.2631	-0.1889
Pyrophacus sp.	-0.4194	**0.5014**	0.3709	0.6596
Scrippsiella sp.	**-0.6256**	-0.2238	-0.1128	0.0574
Cryptophyta	**0.7498**	-0.3218	-0.4345	0.1154
NanoEuk	**0.6491**	-0.4180	-0.4407	0.1613
PicoEuk	**0.8787**	-0.1557	-0.1498	0.1512
Cyanobacteria	**-0.5851**	0.2801	0.3576	-0.1657
Bacteria	**-0.8356**	-0.1805	-0.4241	0.1272

Table S6: Retention times for Cx-HSL, oxo-Cx-HSL and OH-HSL. Predictions based on retention times curves of AHL standards. NP: Non Predictable. The retention time noted with an asterisk are used to predict the unanticipated AHLs presented in the table S7.

	Retention time (Rt, min)		
Acyl-side chain length (C atoms)	Cx-HSL	oxo-Cx-HSL	OH-Cx-HSL
5	**7.85**	**6.97**	NP
6	8.43	7.56	NP
7	8.83	**8.15**	**8.09**
8	9.27	8.69	8.55
9	9.57	**9.04**	**8.92**
10	9.9	9 .43	9.25
11	10.13	**9.74***	**9.59***
12	10.46	10.04	9.87
13	10.63	**10.33***	**10.15**
14	10.93	10 .56	10.42
15	11.15	**10.83**	**10.63**
16	11.34	11.06	**10.85**
17	**11.49**	**11.27**	**11.05**
18	11.66	11.47	**11.24**

Table S7: Mass spectrometry (UHPL-HRMS/MS) data used for the identification of unanticipated AHLs in *V. mediterranei* strains. Rt: Retention Time. Theoritical mass correspond to the pseudo-molecular ion $[M+H]^+$.

Strain	Rt (min)	Observed mass	Molecular Formula	Delta ppm	Fragmentation	Identification			
						Name	Molecular Formula	Molecular Weight	Theorical Mass
17LN 0615E	9,54	286,2012	C15H28NO4	-0,055	69.071 (51.87), **74.061 (18.46)**, 81.070 (81.33), 83.086 (41.72), 93.070 (33.08), 95.086 (100.00), **102.055 (52.81)**, 107.086 (32.94), 109.101 (40.91), 121.101 (67.63), 149.132 (12.43), 170.057 (20.82), 287.201 (15.08)	OH-C11-HSL	C15H27NO4	285,1940	286,2013
	10,26	312,2168	C17H30NO4	-0,135	69.071 (9.79), 71.086 (6.62), **74.061 (36.96)**, 81.070 (13.35), 83.086 (6.35), 95.086 (44.97), **102.055 (100.00)**, 107.087 (24.97), 109.101 (10.05), 121.101 (18.36), 135.117 (17.34), 185.071 (64.95), 211.169 (59.48), 312.276 (14.58)	OXO-C13-HSL	C17H29NO4	311,2097	312,2169
2LS 0615E	9,55	286,2011	C15H28NO4	-0,145	69.071 (14.64), **74.061 (22.24)**, 81.070 (17.80), 83.086 (20.68), 93.070 (11.82), 95.086 (25.37), **102.055 (100.00)**, 107.086 (12.88), 109.101 (14.28), 121.101 (12.49), 149.132 (11.29), 170.057 (26.13), 287.201 (18.21)	OH-C11-HSL	C15H27NO4	285,1940	286,2013
	10,26	312,2174	C17H30NO4	1,426	69.0701 (14.76), 71.086 (16.86), **74.061 (15.64)**, 81.070 (27.04), 83.086 (17.96), 95.086 (46.07), **102.055 (42.05)**, 107.086 (16.36), 109.101 (20.61), 121.101 (15.26), 135.117 (16.86), 185.071 (100.00), 211.169 (21.80), 312.113 (21.79)	OXO-C13-HSL	C17H29NO4	311,2097	312,2169
21LN 0615E	9,54	286,2011	C15H28NO4	-0,145	69.071 (13.52), **74.061 (21.23)**, 81.070 (14.69), 83.086 (16.68), 93.070 (9.02), 95.086 (13.95), **102.055 (100.00)**, 107.086 (10.64), 109.101 (17.15), 121.101 (7.24), 149.132 (11.28), 170.057 (23.23), 287.201 (8.34)	OH-C11-HSL	C15H27NO4	285,1940	286,2013
	10,26	312,2169	C17H30NO4	-0,015	69.070 (25.41), 71.086 (12.84), **74.061 (12.12)**, 81.070 (30.68), 83.086 (27.48), 95.086 (36.26), **102.055 (65.45)**, 107.086 (15.44), 109.101 (20.68), 121.101 (15.93), 135.117 (11.54), 185.071 (17.43), 211.169 (48.71), 312.325 (12.16)	OXO-C13-HSL	C17H29NO4	311,2097	312,2169
	9,71	284,1859	C15H26NO4	0,275	**56.050 (26.96)**, 67.055 (33.74), 69.070 (34.97), 81.070 (73.61), 83.086 (48.93), 93.070 (47.13), 95.086 (75.94), 97.102 (25.44), **102.055 (17,93)**, 107.086 (55.85), 109.101 (48.94), 114.962 (30.51), 119.086 (26.78), 121.101 (39.53), 143.073 (100.00), 235.632 (31.38), 244.637 (95.08), 253.643 (40.17), 283.241 (28.80), 284.295 (77.62)	OXO-C11-HSL	C15H25NO4	283,1784	284,1856
9LS 0615E	9,54	286,2012	C15H28NO4	-0,085	69.071 (14.64), **74.061 (22.24)**, 81.070 (17.80), 83.086 (20.68), 93.070 (11.82), 95.086 (25.37), **102.055 (100.00)**, 107.086 (12.88), 109.101 (14.28), 121.101 (12.49), 149.132 (11.29), 170.057 (26.13), 287.201 (18.21)	OH-C11-HSL	C15H27NO4	285,1940	286,2013
	10,26	312,2169	C17H30NO4	-0,015	69.070 (38.02), 71.086 (22.36), **74.061 (18.54)**, 81.070 (100.00), 83.086 (36.43), 95.086 (93.55), **102.055 (18.80)**, 107.086 (22.81), 109.101 (62.49), 121.101 (25.50), 135.117 (28.01), 185.071 (27.34), 211.169 (20.55), 312.276 (17.86)	OXO-C13-HSL	C17H29NO4	311,2097	312,2169
	9,7	284,1857	C15H26NO4	0,124	**56.050 (15.38)**, 67.055 (29.34), 69.070 (25.92), 81.070 (69.81), 83.086 (34.59), 93.070 (53.28), 95.086 (81.05), 97.102 (18.33), **102.055 (25.72)**, 107.086 (58.46), 109.101 (39.87), 114.962 (33.54), 119.086 (23.16), 121.101 (42.96), 143.073 (100.00), 235.632 (19.63), 244.637 (74.43), 253.643 (36.27), 283.241 (22.64), 284.295 (73.19)	OXO-C11-HSL	C15H25NO4	283,1784	284,1856

Table S8: Mass spectrometry (UHPL-HRMS/MS) data used for the identification of anticipated AHLs in *V. mediterranei* strains. Rt: Retention Time. Theoritical mass correspond to the pseudo-molecular ion $[M+H]^+$.

AHL Standard	Molecular Formula	Theorical Mass	Observed Mass	Rt (min)
C4-HSL	$C_8H_{13}NO_3$	172.0968	172.0968	5.26
C6-HSL	$C_{10}H_{17}NO_3$	200.1281	200.1281	8.43
OXO-C6-HSL	$C_{10}H_{15}NO_3$	214.1074	214.1072	7.56
C7-HSL	$C_{11}H_{19}NO_3$	214.1438	214.1440	8.83
C8-HSL	$C_{12}H_{21}NO_3$	228.1594	228.1594	9.27
OXO-C8-HSL	$C_{12}H_{19}NO_4$	242.1387	242.1381	8.69
OH-C8-HSL	$C_{12}H_{21}NO_4$	244.1543	244.154	8.55
C9-HSL	$C_{13}H_{23}NO_3$	242.1751	242.1748	9.57
C10-HSL	$C_{14}H_{25}NO_3$	256.1907	256.1907	9.90
OXO-C10-HSL	$C_{14}H_{23}NO_4$	270.1700	270.1699	9.43
OH-C10-HSL	$C_{14}H_{25}NO_4$	272.1856	272.1856	9.25
C11-HSL	$C_{15}H_{27}NO_3$	270.2064	270.2063	10.13
C12-HSL	$C_{16}H_{29}NO_3$	284.2220	284.2220	10.46
OXO-C12-HSL	$C_{16}H_{27}NO_4$	298.2013	298.2013	10.04
OH-C12-HSL	$C_{16}H_{29}NO_4$	300.2169	300.2169	9.87
C13-HSL	$C_{17}H_{31}NO_3$	298.2377	298.2377	10.63
C14-HSL	$C_{18}H_{33}NO_3$	312.2533	312.2533	10.93
C14:1-HSL	$C_{18}H_{31}NO_3$	310.2377	310.2370	10.51
OXO-C14:1-HSL	$C_{18}H_{29}NO_4$	324.2169	324.2170	10.23
OXO-C14-HSL	$C_{18}H_{31}NO_4$	326.2326	326.2322	10.56
OH-C14-HSL	$C_{18}H_{33}NO_4$	328.2482	328.2482	10.42
C15-HSL	$C_{19}H_{35}NO_3$	326.2690	326.2689	11.15
C16-HSL	$C_{20}H_{37}NO_3$	340.2846	340.2846	11.34
C16:1-HSL	$C_{20}H_{35}NO_3$	338.2690	338.2704	10.93
OXO-C16:1-HSL	$C_{20}H_{33}NO_4$	352.2482	352.2497	10.61
C18-HSL	$C_{22}H_{42}NO_3$	368.3159	368.3155	11.66
C18:1-HSL	$C_{22}H_{39}NO_3$	366.3003	366.3003	11.40

Table S9: Potential candidate proteins for AHL production in G1 *V. mediterranei* isolates 17 LN0615E and 21 LS0615E with their accession numbers. The 15 proteins are showing 100% identity between the two strains.

Predicted proteins	17LN0615E	21LN0615E
N-acetyltransferase	PRQ67551.1	PCD90480.1
long-chain fatty acid--CoA ligase	PRQ66386.1	PCD88787.1
lauroyl-Kdo(2)-lipid IV(A) myristoyltransferase	PRQ66024.1	PCD86675.1
GNAT family N-acetyltransferase	PRQ67405.1	PCD87616.1
lipid A biosynthesis lauroyl acyltransferase	PRQ66025.1	PCD86676.1
lipid A biosynthesis acyltransferase	PRQ68200.1	PCD89439.1
Predicted hydrolase or acyltransferase	PRQ65458.1	PCD89625.1
Predicted hydrolase or acyltransferase	PRQ67698.1	PCD90333.1
GNAT family N-acetyltransferase	PRQ66292.1	PCD86936.1
N-acetyltransferase	PRQ66291.1	PCD86937.1
N-acetyltransferase	PRQ68639.1	PCD89064.1
GNAT family N-acetyltransferase	PRQ66253.1	PCD86975.1
N-acetyltransferase	PRQ66250.1	PCD86978.1
N-acetyltransferase	PRQ66266.1	PCD86962.1
N-acetyltransferase	PRQ68671.1	PCD89096.1